CHIN. PHYS. LETT. Vol. 35, No. 10 (2018) 104202

Tunable Supercontinuum Generated in a Yb^{3+}-Doped Microstructure Fiber Pumped by Ti:Sapphire Femtosecond Laser *

Wei Wang(王伟)[1,2,3**], Fan-Chao Meng(孟凡超)[1,3], Yuan Qing(卿源)[1,3], Shi Qiu(邱石)[1,3], Ting-Ting Dong(董婷婷)[1,3], Wei-Zhen Zhu(朱维震)[1,3], Yu-Ting Zuo(左玉婷)[1,3], Ying Han(韩颖)[1,3], Chao Wang(王超)[4], Yue-Feng Qi(齐跃峰)[1,3], Lan-Tian Hou(侯蓝田)[1,3]

[1]*School of Information Science and Engineering, Yanshan University, Qinhuangdao 066004*
[2]*Jiangsu Key Laboratory of Meteorological Observation and Information Processing, Nanjing University of Information Science and Technology, Nanjing 210000*
[3]*Key Laboratory for Special Fiber and Fiber Sensor of Hebei Province, Qinhuangdao 066004*
[4]*Intelligence and Information Engineering college, Tangshan University, Tangshan 063000*

(Received 26 June 2018)

We experimentally demonstrate that a tunable supercontinuum (SC) can be generated in a Yb^{3+}-doped microstructure fiber by the concept of wavelength conversion with a Ti:sapphire femtosecond (fs) laser as the pump. Experimental results show that an emission light around 1040 nm in an anomalous dispersion region is first generated and amplified by fs pulses in the normal dispersion region. Then, SC spectra from 1100 to 1380 nm and 630 to 840 nm can be achieved by combined effects of higher-order soliton fission and Raman soliton self-frequency shift in the anomalous dispersion region and self-phase modulation, dispersive wave, and four-wave mixing in the normal dispersion region. It is also demonstrated that the 20 nm change of pump results in a 280 nm broadband shift of soliton and the further red-shift of soliton is limited by OH^- absorption at 1380 nm.

PACS: 42.65.−k, 42.65.Tg, 42.65.Wi, 42.81.−i DOI: 10.1088/0256-307X/35/10/104202

Supercontinuum (SC) has attracted a good deal of interest since it was reported because it can find extensive usages in pulse compression, spectral analysis, optical communication, frequency metrology, and so on. For SC generation, it is one of the commonly used concepts to pump highly nonlinear microstructure fibers (MSFs) in their anomalous dispersion region by Ti:sapphire femtosecond (fs) laser. One advantage of the above scheme is that broadband SC can be achieved within only several tens of centimeters of fiber length by combination both merit of high peak power of fs pulses and the nonlinear effects in anomalous dispersion region of MSFs, such as high-order soliton fission, Raman soliton self-frequency shift (SSFS) and dispersive wave (DW).[1] More importantly, a wideband tunable spectrum can be easily achieved by simply adjusting the pump wavelength of the Ti:sapphire fs laser. Tu *et al.*[2] experimentally demonstrated narrowband DW with a tuning range of 485–690 nm when commercial nonlinear MSFs of 7.2 and 8.3 cm are pumped by Ti:sapphire fs laser from 860 to 1020 nm. Minkovich *et al.*[3] reported a tunable broadband SC from visual wavelengths up to 1600 nm in a homemade MSF with irregular claddings by tuning the Ti:sapphire laser in the range of 700–950 nm. Yuan *et al.*[4] showed that anti-Stokes waves tunable from 669 to 612 nm can be obtained when fs pulses with center wavelength of 810–840 nm are coupled into a 30 cm MSF. However, to tune the anomalous dispersion region to the output spectrum of Ti:sapphire fs laser, it is essential that the MSFs have a very high air-filling fraction with thin silica walls and a small core. This results in a low coupling efficiency of pump and makes the MSFs susceptible to optical damage, which further limits the spectral power density (SPD) of the SC.

An alternative method is to take advantage of the wavelength conversion and optical amplification of rare-earth doped MSFs, usually Yb^{3+}-doped MSFs. In these experiments, the pump laser and the emission peak of Yb^{3+} ions are located in the normal and anomalous dispersion region of Yb^{3+}-doped MSFs, respectively. The stimulated radiation in the anomalous dispersion region is first amplified by pumping in the normal dispersion region. Then, it is employed in subsequent SC generation. In Ref. [5], continuous wave (CW) at 975 nm and nanosecond pulses at 1062 nm are simultaneously coupled into a Yb^{3+}-doped double-clad MSF and a noticeable increase of the SPD level of SC in the 500–900 nm range are experimentally demonstrated. Baselt *et al.*[6] found that the spectral flatness of SC can be improved in 1130–1370 nm when CW at 975 nm and nanosecond pulse at 1064 nm are simultaneously pumping the Yb^{3+}-

*Supported by the National Natural Science Foundation of China under Grant No 61735011, the Natural Science Foundation of Hebei Province under Grant Nos F2016203389 and F2018105036, the Science and Technology Research Project of College and University in Hebei Province under Grant No BJ2017108, the Open Subject of Jiangsu Key Laboratory of Meteorological Observation and Information Processing under Grant No KDXS1107, and the Science and Technology Project of Tangshan City under Grant No 17130257a.

**Corresponding author. Email: wangwei@ysu.edu.cn

© 2018 Chinese Physical Society and IOP Publishing Ltd

doped MSF. A method to overcome the power threshold during the SC generation is also studied.[7] Using the Yb^{3+}-doped MSF with dual wavelengths pumped at 976 and 1064 nm, an all-fiber SC source of spectral range between 1100 nm to 1380 nm has been built up by Baselt *et al.*[8] The SC generated in Yb^{3+}-doped MSF has already been used for coherent anti-Stokes Raman scattering spectroscopy.[9] For all the research mentioned above, a diode laser at 976/975 nm is used as the pump to ensure the absorption and conversion efficiency of Yb^{3+}-doped MSF. The wavelength of the pump cannot be tuned broadly to trim the SC, compared with SC generated through Ti:sapphire fs laser. Moreover, a seed laser at 1064 nm must be simultaneously coupled into the Yb^{3+}-doped MSF together with the pump to improve the quality of the SC, which also increases the complexity of the system.

In this Letter, SC is generated in a Yb^{3+}-doped MSF by a single pump of Ti:sapphire fs laser. Firstly, the absorptive and emissive properties of the Yb^{3+}-doped MSF are measured when the laser is mode-unlocked. Then, the influences of pump power and fiber length on SC are studied and analyzed. Finally, the relation between the red shift of Raman soliton and the pump wavelength is investigated. Experimental results show that high power conversion efficiency can be achieved with a fiber length as short as 0.5 m, and the pump wavelength blue-shifted over 80 nm from the absorption peak of Yb^{3+}. It is also found that wideband tunable Raman soliton of 280 nm can also be achieved by a 20 nm change of pump wavelength. Further blue shift and red shift of SC are limited by absorption of OH^- at 1380 nm.

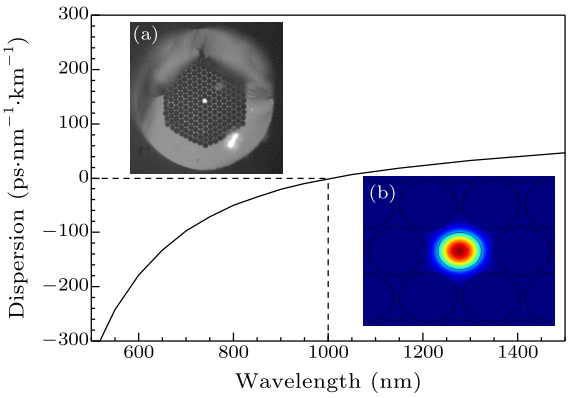

Fig. 1. Dispersion curve of the fundamental mode as a function of wavelength. The inset figures show cross section (a) and simulated fundamental mode (b) of the Yb^{3+}-doped MSF.

The Yb^{3+}-doped MSF used in our experiments is designed and fabricated deliberately to ensure that the output of our Ti:sapphire fs laser (<980 nm) and emission of Yb^{3+} ions (around 1040 nm) are located in normal and anomalous dispersion regions of the fiber, respectively. The cross section of the fabricated Yb^{3+}-doped MSF is shown in the inset (a) of Fig. 1. The measured average air hole to air hole pitch, air hole diameter and diameter of the doped region in the fiber core are 5.03 μm, 4.60 μm, and 3.46 μm, respectively. The Yb^{3+}-doped glass used for the fiber core is prepared under the weight percentage (wt%) of $1.5Yb_2^{3+}O_3$-$3.0Al_2O_3$-$0.5K_2O$-$95.0SiO_2$ and its refractive index is 1.519 at 589 nm measured by an Abbe refractometer. The waveguide dispersion is then numerically simulated by the finite element method with the index of pure silica set as 1.4584 at 589 nm. The total dispersion is calculated as the sum of waveguide and material dispersion, where the material dispersion is obtained by the Sellmeier equation. Figure 1 shows the calculated dispersion curve of the fundamental mode, from which we can see that the zero dispersion wavelength λ_0 locates at 1000 nm. The field distribution of the fundamental mode is also simulated and shown in the inset (b) of Fig. 1. The calculated effective mode area of the fundamental mode is 6.67 μm^2 at λ_0 and is much less than that of Yb-doped fibers used in the fiber laser. The nonlinear coefficient γ will be up to 26 $W^{-1}\cdot km^{-1}$ even if the fiber core is made of pure silica and its value will further increase for our Yb^{3+} ions doped fiber, which indicates that our fiber is a promising medium for SC generation.

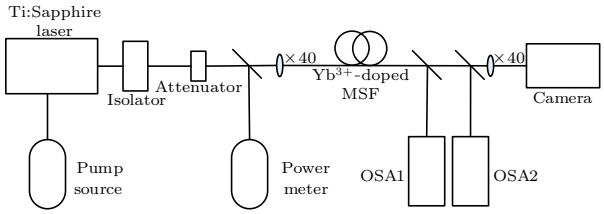

Fig. 2. Experimental setup used for SC generation in the Yb^{3+}-doped MSF.

The experimental setup is shown in Fig. 2. Here fs pulses are generated by a Mira900 Ti:sapphire fs laser with 120 fs width at a repetition rate of 76 MHz. The average output power of the laser is first adjusted by an attenuator. Then, fs pulses are coupled into the fiber by a 40× objective with an estimated coupling efficiency of about 60%. A camera is placed at the back-end of the MSF to ensure that fs pulses are coupled into the fiber core by observing the location of the optical field on the Yb^{3+}-doped MSF. The output spectrum is received and detected by two fiber optical spectrum analyzers (OSA1: Avaspec-256 with spectral range of 200–1100 nm, OSA2: Avaspec-NIR-256 with spectral range of 900–2400 nm). Before the experiments, the responses of the two OSAs have been calibrated by tungsten halogen lamp, thus the entire output spectrum can be obtained by splicing the spectra of two OSAs together.

We first measure the emission spectrum of our Yb^{3+}-doped MSF using 0.30 W CW output of the Ti:sapphire laser at 850, 870 and 890 nm when the laser is mode-unlocked. The tested fiber is 0.5 m and the results are presented in Fig. 3. When Yb^{3+} ions are doped into silica, the ground state $^2F_{7/2}$ splits into

four Stark sublevels and the excited state $^2F_{5/2}$ splits into three Stark sublevels. Thus the Yb^{3+}-doped fiber has a wide absorption band of 800–1064 nm with an absorption peak and sub-peak around 975 nm and 915 nm, and a wide emission band of 970–1200 nm with an emission peak and sub-peak around 975 nm and 1030 nm.[10,11] From Fig. 3, it can be seen that the emission band of our Yb^{3+}-doped MSF is centered at 1040 nm with a full width at half maxima (FWHM) of about 15 nm, and it does not shift with the pump wavelength. It is also found that the absorption and emission efficiency is obviously lowered if the central wavelength of the pump moves further away from the absorption peak at 975 nm. The emission around 1040 nm is negligible if the pump wavelength is shorter than 850 nm. However, the Yb^{3+}-doped MSF still shows excellent wavelength conversion efficiency with the pump at 890 nm, which is blue-shifted over 80 nm from the emission peak at 975 nm.

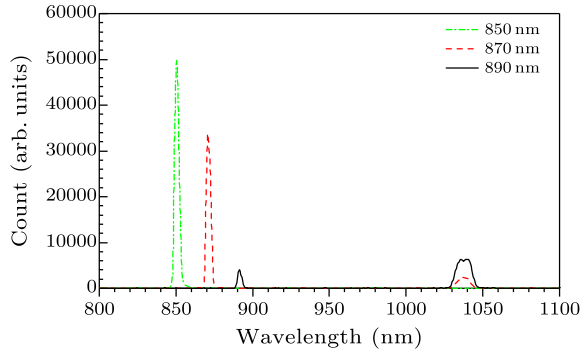

Fig. 3. Emission spectrum of the Yb^{3+}-doped MSF when pump wavelengths are 890 nm (solid line), 870 nm (dashed line), and 850 nm (dash-dotted line), respectively.

Then, the SC generation in the Yb^{3+}-doped MSF is studied. Firstly, the Yb^{3+}-doped MSF is cut into a length of 1.35 m, the central wavelength of fs pulse is set at 890 nm, and the average power of fs pulses P_{pump} is increased from 0.15 W to 0.40 W in Fig. 4. The inset of Fig. 4(a), which is a photo of MSF's back-end cross section, clearly shows that the optical field is located in the Yb^{3+}-doped core. From Fig. 4(a), it is found that the pump centered at 890 nm has been depleted and there are two new spectra appearing in the normal and anomalous dispersion regions of the fiber, respectively. The two newly generated spectra and pump do not satisfy the condition of energy conservation and are not the results of four-wave mixing (FWM). Actually, the blue-shifted spectrum in the range of 804–858 nm is generated by self-phase modulation (SPM). Instead of symmetrical broadening around the pump, the spectrum longer than 860 nm is completely absorbed by Yb^{3+}-doped MSF. As to light in the anomalous dispersion region, it is located in the emission band of our Yb^{3+}-doped MSF and there is no sign of red-shifted soliton. This can be explained by the fact that optical energy at 1040 nm is built up gradually along the fiber length and it is too weak to generate a Raman soliton with a pump of 0.15 W. If the P_{pump} increases from 0.15 W to 0.18 W (Fig. 4(b)), there is a soliton appearing in an anomalous dispersion region and it is further red-shifted to 1120 nm with DW appearing at around 768 nm. However, as seen from Fig. 3, if the CW laser is used as pump, there will still be no sign of soliton even if the pumping power of 0.30 W is much higher than P_{pump} of 0.18 W used in Fig. 4(b). Thus the nonlinear effects in Fig. 4(b) can be explained to come from an ultrashort pulse as a single pump, the spontaneous emission around 1040 nm is initially generated and also evolves into ultrashort pulses because it is amplified and trapped by the fs pump to avoid time-domain broadening, which accounts for subsequent red-shifted soliton and DW. Further increasing P_{pump} to 0.20 W (Fig. 4(c)), a second order soliton is generated and splits to two fundamental Raman solitons at 1106 and 1215 nm, with corresponding DWs peaked at 764 and 717 nm. The peak at 700 nm is the anti-Stokes signal of a degenerate FWM with pump at 890 nm and Stokes line at 1215 nm. When P_{pump} reaches 0.40 W (Fig. 4(d)), SC ranging from 1100 to 1380 nm is generated by combined effects of higher-order soliton fission and Raman SSFS in the anomalous dispersion region. However, the absorption of OH^- at 1380 nm prevents further red-shifting of Raman soliton and broadening of the SC. The SC ranging from 630 to 840 nm is generated by combined effects of SPM, DW, and FWM in the normal dispersion region. The entire SC is divided into two separate parts, which is due to the absorption of the Yb^{3+}-doped MSF. The inset of Fig. 4(d) shows a photo of the far field distribution of SC output, which is circular and Gaussian distributed.

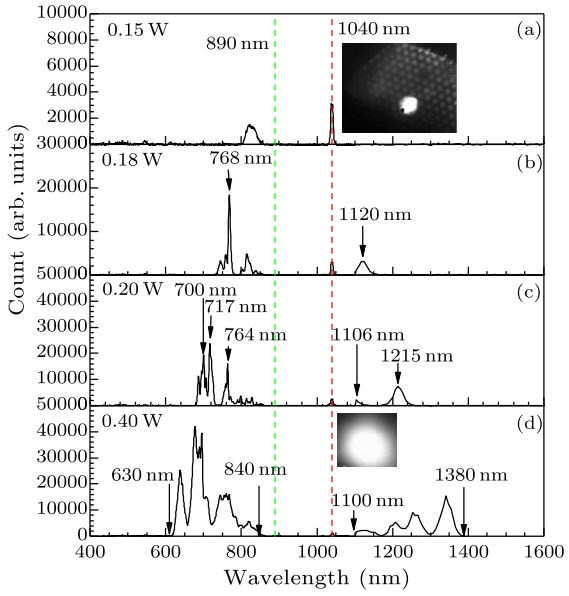

Fig. 4. The SC of Yb^{3+}-doped MSF when the pump powers are (a) 0.15 W, (b) 0.18 W, (c) 0.20 W, and (d) 0.40 W, respectively.

As the main purpose of this work is focused on

investigating the physical mechanism of SC generation in Yb^{3+}-doped MSF pumping by a single fs laser, the SPD of output SC is not recorded and optimized in our experiments. However, to better quantify the performance of our experiments, a new parameter, namely apparent conversion efficiency η, is defined as $\eta = 1 - P_0/P_{\text{out}}$, where P_{out} and P_0 stands for the power of the entire output spectrum and residual output pump, respectively. In our experiments, residual fs pulse of Ti:sapphire femtosecond laser around 890 nm with 10 nm width and Yb^{3+} emission around 1040 nm with 20 nm width are both considered as the residual pump, as wavelength conversion and optical amplification of Yb^{3+} at 1040 nm also behaves as a pump to be employed in subsequent SC generation. Though the output power is not recorded, P_0/P_{out} can still be readily calculated by integrating the output of OSAs. According to the above definition, η is only 63.8% with 0.15 W pump in Fig. 4(a). This value reaches as high as 99.7% when the pump power increases to 0.40 W in Fig. 4(d), from which we can find that the residual pump around 890 and 1040 nm has almost depleted. However, it should be noted that the actual wavelength conversion efficiency of the entire system is much lower than the value we obtained above, because the coupling loss between the pump and MSF, the confinement loss of the MSF and the absorption loss of Yb^{3+} and OH^- are neglected in our computation.

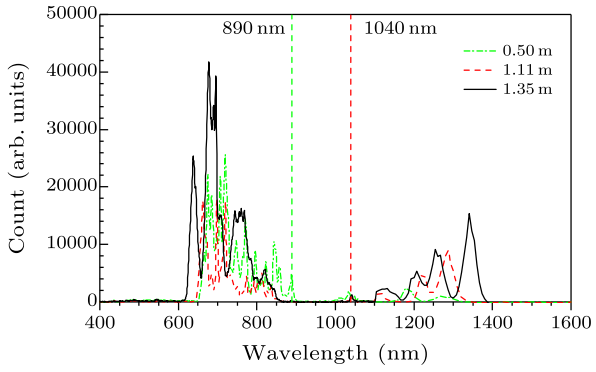

Fig. 5. The SC of Yb^{3+}-doped MSF when the fiber lengths are 1.35 m (solid line), 1.11 m (dashed line), and 0.50 m (dot-dashed line), respectively.

Next, the fiber length's influences on SC generation are illustrated in Fig. 5. The fiber length is cut from 1.35 m to 0.5 m with the pump fixed at 890 nm and 0.40 W. As mentioned above, to generate SC by concept of wavelength conversion, the signal light around 1040 nm needs to be first generated and amplified along the fiber length by pumping. From Fig. 5, it is clearly seen that the red and blue frontiers of SC move further outward with longer fiber length. However, with fiber length as short as 0.50 m, the optical power at 890 nm and 1040 nm has almost been converted to SC, which demonstrates that highly efficient wavelength conversion and SC generation are feasible in Yb^{3+}-doped MSF with single ultrashort pulse pumping.

Finally, we prove that the Raman soliton generated in this experiment can be tuned by adjusting the output wavelength of Ti:sapphire fs laser in Fig. 6. The fiber has a length of 1.35 m and the average power of the pump is set as 0.40 W. From Fig. 6, it is found that there is no soliton presented if the central wavelength of the pump is 850 nm because of the low absorption of Yb^{3+} ions at that wavelength. If the central wavelength of the pump is changed from 870 to 890 nm, the furthest red-shifted soliton can be flexibly tuned from 1100 nm to 1380 nm, that is, a 20 nm change of pump results in a 280 nm broadband shift of soliton. Further red-shift of the Raman soliton is limited by the absorption of OH^- at 1380 nm even if the pump exceeds 890 nm. Considering that the output wavelength of the most commercial Ti:sapphire fs lasers can easily reach 1000 nm, we believe that a wideband tunable light source based on the Raman soliton is achievable, only if lower water peak Yb^{3+}-doped MSF can be fabricated by optimizing the production process.

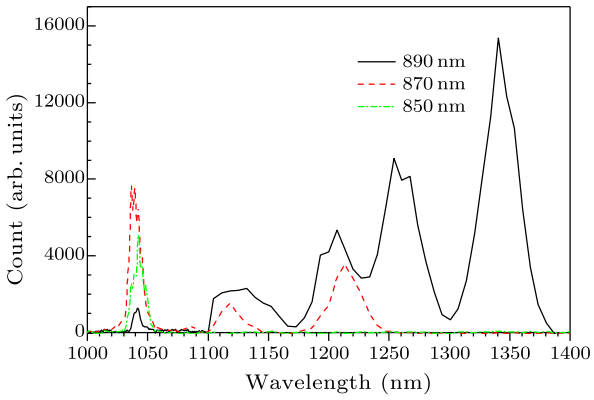

Fig. 6. Raman solitons generated when the pump wavelengths are 890 nm (solid line), 870 nm (dashed line), and 850 nm (dash-dotted line), respectively.

In conclusion, a Yb^{3+}-doped MSF has been fabricated and tunable SC generated in this MSF has been experimentally demonstrated by Ti:sapphire fs laser as the pump. The emission of Yb^{3+} around 1040 nm, which is located in an anomalous dispersion region of the fiber, is first generated by wavelength conversion of the pump in the normal dispersion region and amplified along the fiber length. Then, the spectrum is broadened subsequently by the combined effects of higher-order soliton fission and Raman SSFS in the anomalous dispersion region and SPM, DW, and FWM in the normal dispersion region. Experimental results show that highly efficient wavelength conversion is feasible with fiber length as short as 0.50 m even the pump wavelength is blue-shifted over 80 nm from an absorption peak of Yb^{3+}. When the average pump power and fiber length reach 0.40 W and 1.35 m, SC from 1100 to 1380 nm and 630 to 840 nm is obtained

with pump at 890 nm. Through the change of the pump wavelength, the tunability of the Raman soliton is also investigated. It is found that the furthest red-shifted soliton can be flexibly tuned from 1100 nm to 1380 nm when the central wavelength of the pump is changed from 870 to 890 nm. The absorption of OH^- at 1380 nm prevents further red-shifting of the Raman soliton and broadening of the SC.

References

[1] Herrmann J, Griebner U, Zhavoronkov N, Husakou A, Nickel D, Knight J C, Wadsworth W J, Russell P S J and Korn G 2002 *Phys. Rev. Lett.* **88** 173901

[2] Tu H H and Boppart S A 2009 *Opt. Express* **17** 9858

[3] Minkovich V P, Pereira M V, Villatoro J, Myslivets E, Sotsky A B, Dzen I S, Illarramendi M A and Zubia J 2016 *J. Lightwave Technol.* **34** 4387

[4] Yuan J H, Kang Z, Li F, Zhou G Y, Zhang X T, Mei C, Sang X Z, Wu Q, Yan B B, Zhou X, Zhong K P, Wang K R, Yu C X, Lu C, Tam H Y and Wai P K A 2017 *Sci. Rep.* **7** 9224

[5] Roy A, Leproux P, Roy P, Auguste J L and Couderc V 2007 *J. Opt. Soc. Am.* B **24** 788

[6] Baselt T, Taudt C, Nelsen B, Lasagni A F and Hartmann P 2016 *Proc. SPIE* **9731** 97310L

[7] Baselt T, Taudt C, Nelsen B, Lasagni A F and Hartmann P 2017 *Opt. Eng.* **57** 021207

[8] Baselt T, Taudt C, Nelsen B, Lasagni A F and Hartmann P 2017 *Proc. SPIE* **10088** 100880E

[9] Louot C, Shalaby B M, Capitaine E, Hilaire S, Leproux P, Pagnoux D and Couderc V 2016 *IEEE Photon. Technol. Lett.* **28** 2011

[10] Barua P, Sekiya E H, Saito K and Ikushima A J 2008 *J. Non-Cryst. Solids* **354** 4760

[11] Pask H M, Carman R J, Hanna D C, Tropper A C, Mackechnie C J, Barber P R and Dawes J M 1995 *IEEE J. Sel. Top. Quantum Electron.* **1** 2